PEDOGEOCHEMICAL SURVEY FOR URANIUM MINERALIZATION IN PARTS OF IGARRA SCHIST BELT, SOUTHWESTERN NIGERIA

Adepoju, M. O.[1#], Okonkwo, C. T. [1] and Bolarinwa, A. T.[2]

[1]Department of Applied Geology, Federal University of Technology, Akure, Nigeria
[2]Department of Geology, University of Ibadan, Ibadan, Nigeria
[#]**Corresponding author's Email and phone number:** moadepoju@futa.edu.ng; Tel: 08034722855

ABSTRACT

Pedogeochemical survey for uranium mineralization in Dagbala-Atte district, Igarra schist belt, southwestern Nigeria was carried out. The concentrations of As, Au, Fe, Mn, Mo, Ni, Pb, Se, U and V in the residual soils were subjected to univariate and multivariate analyses and plotted on geochemical distribution maps to delineate possible U-mineralization areas. Histograms and box plots showed the elements are log-normally distributed with threshold values of 9.47 %, 10.8, 1589, 2.98, 45.6, 31.0, 0.68, 8.59, 122 ppm and 10.6 ppb, respectively for Fe, As, Mn, Mo, Ni, Pb, Se, U, V and Au. Correlation matrix revealed a strong correlation between U and each of Fe, Mo and Pb indicating close primary association among these four elements. Factor analysis revealed association of U, Mo and Pb implying possible occurrence of U in the granitic rocks of the area. Geochemical maps showed that the strongest U anomaly occurred in the northeastern part of the district that is underlain by granitic gneisses with numerous unmapable granite-pegmatite veins, which possibly are the host of the U mineralization. Copious geological study of these granite-pegmatite veins is recommended.

Keywords: Anomaly, box plots, correlation matrix, geochemical distribution map, uranium mineralization.

INTRODUCTION

Pedogeochemical survey, which is premised on the fact that buried mineral deposits in certain areas are marked by geochemical features in soils overlying the mineralized area, is relatively new among the exploration techniques used for the discovery of uranium deposits. The development of geochemical soil survey has been retarded by the popularity and success of the more widely used radiometric methods that detect and map natural radioactive emanations (γ ray) from rock and soil; and hydrogeochemical methods that made use of solution properties of uranium. Nevertheless pedogeochemical survey for uranium has been applied with success all over the world by a number of workers including Zang, *et al.*, 2020; Appleton *et al.*, 2013; Power *et al.*, 2012; Chaudry *et al.*, 2001.

In Nigeria, uranium has been reported to occur as sandstone hosted and vein-type mineralization (Adekanmi *et al.*, 2007). The latter has been reported to occur in the migmatites and granitoids in the Gubrunde, Kanawa, Ghumchi, Mika and Monkin–Maza deposits (Adekanmi *et al.*, 2007; Funtua and Okujeni, 1996; Ige *et al.*, 1994) and

there is no reason to believe it may not occur in other areas underlain by crystalline rocks in Nigeria.

Adepoju and Adekoya (2011, 2008) carried out reconnaissance geochemical stream sediment survey of Orle drainage system that drains substantially Igarra Schist Belt. This study revealed anomalous concentration of uranium with some other metals in the stream sediments around Dagbala and Atte areas compelling follow-up studies. The diverse geological settings of uranium deposits (IAEA 2001) makes Igarra schist belt to have high potentials of the presence of this metal. The present study is a follow-up soil geochemical survey designed to explore for uranium mineralization in the more promising Dagbala-Atte District of Igarra Schist Belt, southwestern Nigeria (Fig. 1). It aims at employing trace-element geochemistry of residual soil (pedogeochemical survey) to locate areas underlain by rock(s) with possible uranium mineralization in the district. Dagbala-Atte District is located within latitudes 7° 10' and 7° 21'N and longitudes 6° 09' and 6° 17'E and covers an area of about 285 km^2 (Figure 2).
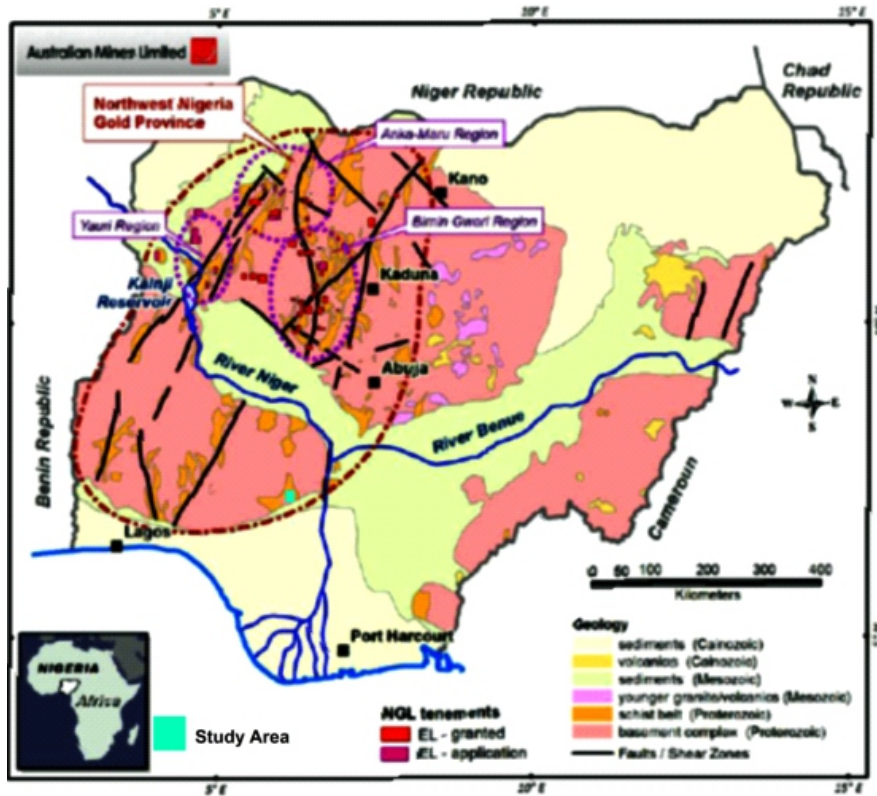
Figure 1. Geological map of Nigeria showing the location of Dagbala-Atte District.
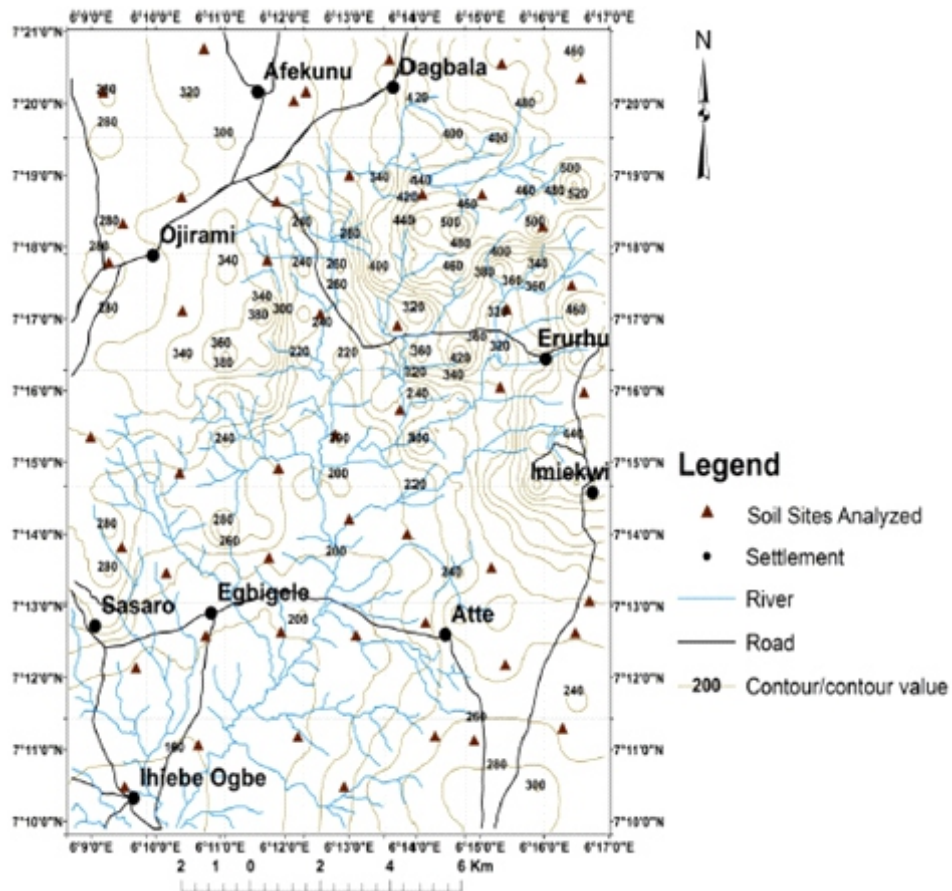

Figure 2 Topographical and drainage map of Dagbala-Atte District showing the locations of soil samples used for this study.

GEOLOGICAL SETTING

Igarra Schist Belt comprises essentially low-grade deformed pelitic to semi-pelitic schists, marbles, calc-silicate gneiss, quartzites and polymictic metaconglomerates (Odeyemi 1988; Egbuniwe and Ocan 2004). The schist belt is surrounded by the older Basement Complex rocks (i.e. the gneisses and migmatites) believed to be of Archean to Paleoproterozoic age (Hockey *et al*. 1986; Dada 2006). Both the metasediments and the older basement rocks were intruded by the Pan African granites (also known as the Older Granites) represented by the lgarra batholith. Minor felsic and mafic intrusives, including pegmatites, aplite, syenite, lamprophyre and dolerite cut-cross the Pan African granites and the pre-existing rocks. The rock suite in the eastern portion of Dagbala-Atte district is dominated by granitic gneisses while the western part is composed mainly of metasediments (Figure 3). These two contrasting lithologies are separated by a narrow zone of silicified, sheared rock (Adepoju, 2017). The metasedimentary assemblage consists of quartz-biotite, garnet-biotite and mica schists with minor metaconglomerate, quartzites and marble. Both the metasediments and the granitic gneisses are intruded by porphyritic Pan African granite. All the rock types are intensely weathered to varying degrees under the prevailing hot and humid tropical climatic conditions producing ubiquitous residual soil profiles.
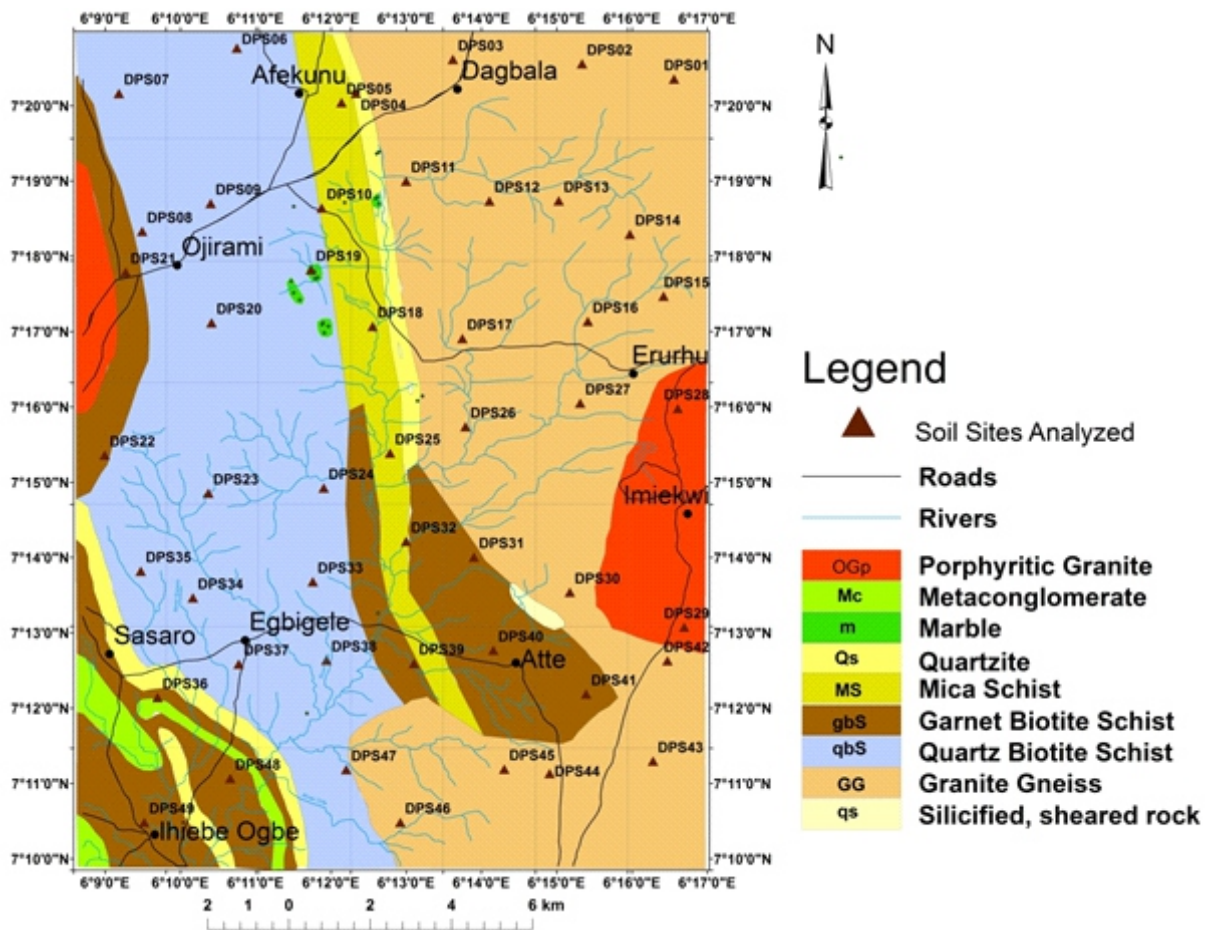

Figure 3. Geological map of Dagbala-Atte District showing the 49 grids used in this study.

METHODOLOGY

Sampling of B-horizon of soils in the Dagbala-Atte District was carried out. The Sampling entailed collecting residual soil from the B-horizon of 49 locations within a predetermined grid pattern of Dagbala-Atte District (Figures 2 and 3). The B horizon of a weathering profile is known as zone of illuviation or accumulation (Rose *et al*. 1991; Levinson, 1980). The clay minerals, as well as the Fe and Mn oxides deposited in the horizon are capable of adsorbing metals. The concentration of metals in the B horizon makes it an optimum zone to sample in soil surveys for mineral exploration. Accessibility to this zone for sampling in an area, as in Dagbala-Atte District, is therefore a factor that predisposes the area for mineral exploration using soil survey.

Geochemical analysis of the forty-nine residual soil samples was carried out using the Inductively Coupled Plasma-Mass Spectroscopy method to determine the concentration of ten elements including As, Au, Fe, Mn, Mo, Ni, Pb, Se, U and V. These elements, except Fe and Mn, were selected on the basis of their known affinity for U and usefulness in U exploration (Rose *et al*., 1991) for the different uranium deposit types adequate for the geologic setting of Dagbala-Atte District (Table 1). Fe and Mn were deliberately included to monitor the mobility of the other ones within the secondary environment of the residual soils. Details of the methodology adopted, as well as, the procedure for quantitative and qualitative data analyses were described in Adepoju (2017, 2019) and Adepoju *et al*. (2019).

Quantitative data analysis, including both univariate statistical analysis employing histograms and box plots, and multivariate statistical analysis involving determination of correlation matrix (CM) and factor analysis (FA) were carried out using a software package - Minitab-16. Qualitative analysis involved plotting the relevant geochemical data to generate element distribution map in an ArcGIS environment to show the distribution and concentration of the various elements.

Table 1. The suitable uranium deposit types for the geologic setting of Dagbala-Atte District and the associated pathfinder elements useful in their exploration (from Rose *et al*., 1991).

Uranium Deposit Type	Major components	Associated elements
Uranium vein in granite	U	Mo, Pb, F
Unconformity associated uranium	U	Ni, Se, Au, Pd, As
Sandstone-type U	U	Se, Mo, V, Cu, Pb
Calcrete U	U	V

RESULTS

The concentrations of the ten elements in the residual soils of the Dagbala-Atte District are presented in Table 2. For the univariate statistics, the histograms plotted for the raw concentration values and their logarithmically transformed version for some of the elements are presented in Figure 4. Figure 5 gives the box plots constructed for both the raw and log data of the elements. The descriptive statistics gotten from these plots are presented in Table 3.

For the multivariate statistical analysis, Se is not considered because it contains censored data in more than 30 % of the sampling points. The correlation coefficients of the remaining nine elements are given in Table 4, while the result of FA is presented in Table 5. The geochemical distribution maps plotted for Mo and U are shown in Figure 6 a and b, respectively.

Table 2. Raw Concentrations of Relevant Elements for Exploration of U in Soils of Dagbala-Atte District.

	Longitude	Latitude	As	Au	Fe	Mn	Mo	Ni	Pb	Se	U	V
DPS01	6.27601	7.33925	0.6	1.2	1.9	80	2.25	2.7	9.41	0.2	12.7	12
DPS02	6.25559	7.34263	0.7	1.3	0.87	480	0.34	3.8	8.99	0.2	2.6	12
DPS03	6.22703	7.34360	0.9	1.7	2.64	381	1.21	12.5	14.89	0.2	4.6	54
DPS04	6.20553	7.33612	5.1	4.8	2.64	263	0.98	10.4	10.05	0.4	1.1	47
DPS05	6.20233	7.33403	0.7	2.3	0.83	120	0.17	3.5	4.67	0.1	0.3	17
DPS06	6.17917	7.34610	1.2	2.1	2.12	158	0.33	11.4	8.93	0.2	1	46
DPS07	6.15307	7.33607	0.6	8.3	0.7	107	0.07	4.5	6.24	<0.1	2.1	19
DPS08	6.15820	7.30553	0.3	1.7	0.37	230	0.11	2.2	4.35	0.1	0.3	9
DPS09	6.17338	7.31172	0.3	0.9	0.12	16	<0.01	1.3	1.99	<0.1	0.2	4
DPS10	6.19797	7.31070	0.7	5.6	2.83	296	0.27	30.7	10.47	0.2	0.8	49
DPS11	6.21667	7.31667	214.5	12.5	4.43	21	0.45	10.1	10.74	0.2	2.8	128
DPS12	6.23509	7.31228	0.8	0.5	1.12	673	1.08	3.9	19.23	0.5	5.9	14
DPS13	6.25047	7.31230	0.6	0.5	1.46	279	0.79	3.8	8.21	<0.1	4.2	16
DPS14	6.26623	7.30491	0.5	1.3	1.49	116	0.64	4.7	8.44	0.2	2.4	21
DPS15	6.27367	7.29119	1.2	9.8	3.6	459	2.5	3.9	24.99	0.4	8.5	16
DPS16	6.25689	7.28561	1.9	3.5	5.49	427	2.46	9.6	19.52	0.2	2.3	60
DPS17	6.22911	7.28183	0.6	2.7	2.55	315	0.11	21.1	2.65	<0.1	2.6	42
DPS18	6.20923	7.28452	2.4	8.3	2.1	312	0.55	19.8	7.1	0.3	1.4	40
DPS19	6.19558	7.29703	3.5	1.8	2.21	356	0.15	23.4	8.12	0.3	0.7	45
DPS20	6.17358	7.28531	0.3	0.5	0.35	37	0.04	3.6	4.35	<0.1	0.4	13
DPS21	6.15455	7.29648	0.5	0.7	1.17	386	0.32	7.6	8.23	<0.1	0.7	27
DPS22	6.14990	7.25602	0.5	<0.2	0.66	210	0.15	4	4.4	0.2	0.4	13
DPS23	6.17286	7.24761	1.9	1.2	3.34	502	0.41	36.8	13.6	<0.1	0.9	67
DPS24	6.19840	7.24875	0.7	2.2	1.8	402	0.31	16.9	8.53	0.1	1.2	51
DPS25	6.21308	7.25647	0.1	0.7	0.52	264	0.2	2.8	5.7	0.2	0.9	12
DPS26	6.22980	7.26231	0.7	<0.2	2.5	496	0.3	12.3	9.01	0.4	3.7	45
DPS27	6.25521	7.26753	0.8	0.6	2.16	893	1.08	6.8	16.5	0.2	1.9	23
DPS28	6.27683	7.26634	0.9	2.6	8.12	983	2.16	5.3	20.41	0.2	1.9	34
DPS29	6.27823	7.21795	2	<0.2	3.97	374	1.03	10.5	8.94	<0.1	1	23
DPS30	6.25292	7.22567	0.8	6.6	2.2	268	0.97	7.8	14.88	0.4	1.4	43
DPS31	6.23168	7.23347	1.3	3.8	2.72	286	0.6	20.6	16.03	0.4	2.1	60
DPS32	6.21665	7.23692	0.5	1.4	3.43	288	0.46	28.4	11.9	0.3	1	61
DPS33	6.19598	7.22800	0.9	1.1	2.29	483	0.31	46.2	11.19	0.3	0.9	51
DPS34	6.16945	7.22443	3.5	0.8	2.79	658	0.37	27.8	15.92	0.3	0.7	54
DPS35	6.15790	7.23035	4	0.7	3.6	804	0.38	34	16.17	0.5	0.6	71
DPS36	6.16160	7.20237	0.4	0.4	1.19	208	0.21	9.3	8.59	<0.1	0.4	25
DPS37	6.17962	7.20980	0.5	0.8	0.86	306	0.31	3.8	9.2	<0.1	0.4	16
DPS38	6.19903	7.21065	17.4	1.3	12.33	127	2.82	10.5	15.95	1.1	4.7	128
DPS39	6.21840	7.20993	<0.1	0.4	2.26	382	0.23	21.5	11.71	<0.1	0.9	43
DPS40	6.23597	7.21285	0.5	0.4	1.27	213	0.22	9.6	5.6	<0.1	0.6	21
DPS41	6.25653	7.20315	1.4	<0.2	1.51	296	0.46	5.6	18.83	0.3	2.9	27
DPS42	6.27455	7.21050	0.6	1.2	2.9	1159	0.81	5.6	17.25	<0.1	1.5	22
DPS43	6.27132	7.18831	0.8	5.9	2.13	512	0.74	11.5	14.14	<0.1	2.7	42
DPS44	6.24842	7.18557	0.5	<0.2	1.62	451	0.44	6.3	20.2	0.2	1.5	31
DPS45	6.23840	7.18655	2.6	1.4	5.84	302	1.31	10.9	16.28	0.2	1.8	62
DPS46	6.21537	7.17475	1	0.4	2.39	493	0.23	16.5	26.94	0.2	2.9	48
DPS47	6.20342	7.18643	2.3	0.5	2.09	646	0.78	9	12.41	0.1	1.4	29
DPS48	6.17772	7.18448	0.7	<0.2	1.72	254	0.24	10.9	9.09	0.2	0.5	36
DPS49	6.15867	7.17477	0.4	0.8	1.12	289	0.16	11.6	5.08	<0.1	0.2	25

Longitude and latitude in ^{o}, Au in ppb, other elements in ppm.
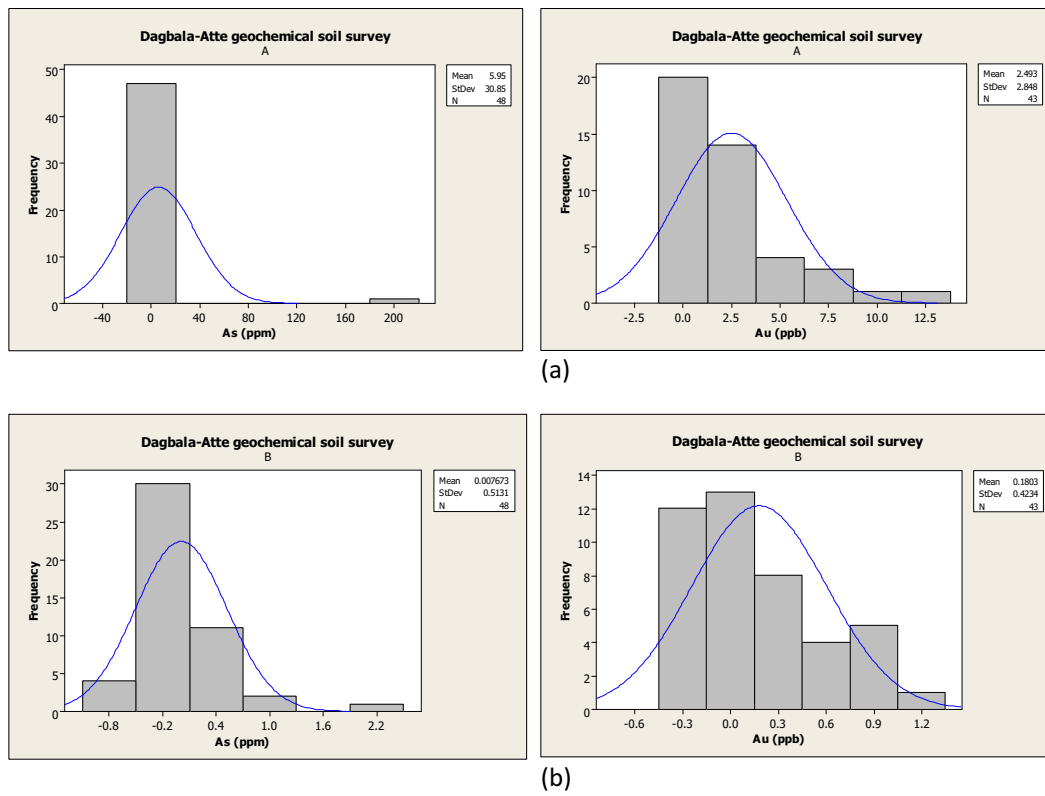
Figure 4. Histograms of (a) raw and (b) Logarithmically transformed concentrations of As and Au in soils of Dagbala-Atte District.
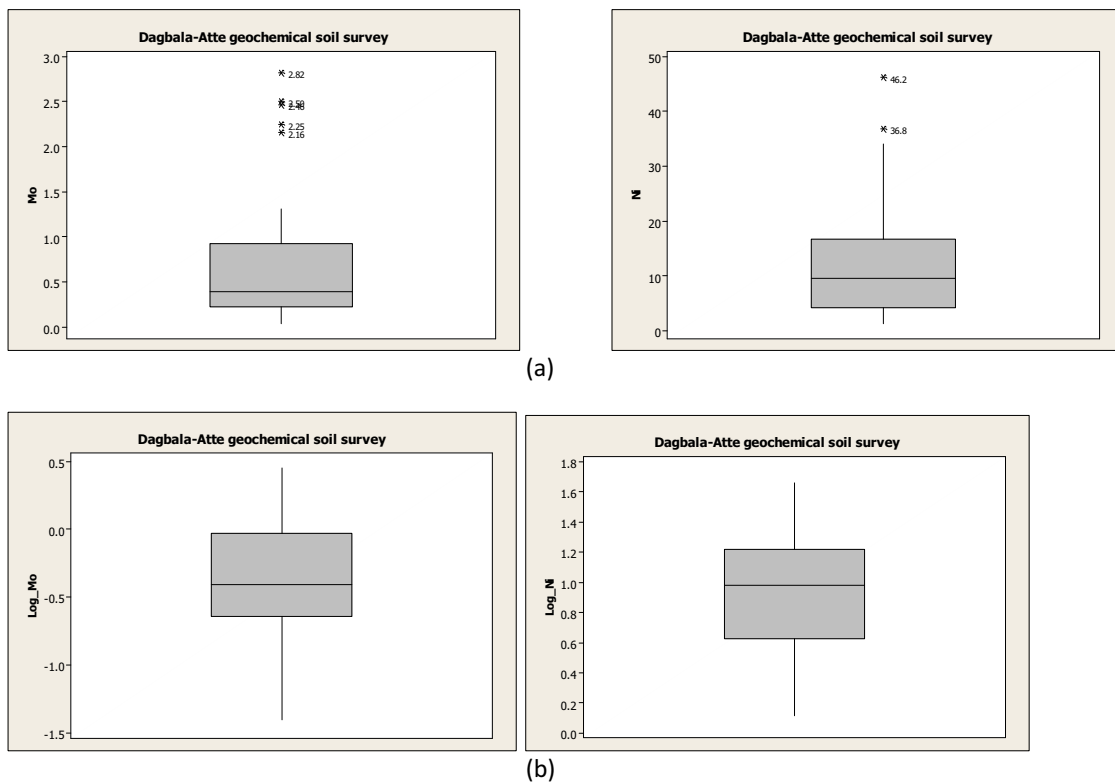

Figure 5 Boxplot of (a) raw and (b) Logarithmically transformed concentrations of Mo and Ni in soils of Dagbala-Atte District.

Table 3: Descriptive statistics of Fe, As, Mn, Mo, Ni, Pb, Se, U, V and Au, in the residual soils of
Dagbala-Atte District.

Ele.	N	Mean	St. Dev.	Min.	Q1	Med.	Q3	Max.	IQR	Thr. 1	Thr. 2
Fe	49	0.265	0.356	-0.921	0.072	0.328	0.449	1.091	0.377	9.47	10.3
As	48	0.008	0.513	-1.000	-0.301	-0.126	0.246	2.331	0.547	10.8	11.6
Mn	49	2.452	0.375	1.204	2.345	2.486	2.683	3.064	0.338	1589	1545
Mo	48	-0.359	0.416	-1.398	-0.638	-0.404	-0.033	0.450	0.606	2.98	7.51
Ni	49	0.950	0.355	0.114	0.628	0.982	1.223	1.665	0.595	45.6	130.4
Pb	49	1.003	0.244	0.299	0.912	1.002	1.204	1.430	0.292	31.0	43.8
Se	34	-0.614	0.222	-1.000	-0.699	-0.699	-0.492	0.041	0.207	0.68	0.66
U	49	0.113	0.410	-0699	-0.155	0.146	0.415	1.104	0.570	8.59	18.6
V	49	1.484	0.300	0.602	1.255	1.532	1.699	2.107	0.444	122	232
Au	43	0.180	0.423	-0.398	-0.155	0.114	0.431	1.097	0.586	10.6	20.5

Table 4: Correlation matrices for Fe, As, Mn, Mo, Ni, Pb, U, V and Au in the residual soils of
Dagbala-Atte District

	As	Au	Fe	Mn	Mo	Ni	Pb	U	V
As	1								
Au	0.331	1							
Fe	0.604	0.225	1						
Mn	-0.097	-0.163	0.442	1					
Mo	0.374	0.178	0.776	0.481	1				
Ni	0.358	0.112	0.603	0.394	0.147	1			
Pb	0.380	0.043	0.695	0.580	0.756	0.312	1		
U	0.290	0.214	0.503	0.185	0.677	-0.022	0.551	1	
V	0.661	0.259	0.819	0.244	0.423	0.820	0.511	0.231	1

Table 5(a): Equamax Rotated Factor Loadings and Communalities

Variable	Factor1	Factor2	Factor3	Communality
As	0.263	-0.522	-0.622	0.728
Au	0.117	-0.107	-0.740	0.573
Fe	0.644	-0.684	-0.159	0.908
Mn	0.504	-0.373	0.647	0.812
Mo	0.916	-0.202	-0.064	0.883
Ni	-0.019	-0.949	0.066	0.905
Pb	0.810	-0.373	0.115	0.808
U	0.840	0.089	-0.262	0.783
V	0.251	-0.900	-0.254	0.937
Variance	3.0156	2.7884	1.5334	7.3374
% Var	0.335	0.310	0.170	0.815

Table 5 (b): Element associations and their Eigen values (%)

Factor	Element associations	Eigen value (%)
1	Mo-U-Pb-Fe-Mn	33.5
2	Ni-V-Fe-As	31.0
3	Au-Mn-As	17.0

Table 6: Background concentration of the analyzed trace elements in soils and their uses in geochemical exploration (after Levinson, 1980 and Rose *et al.*, 1991).

Elements	Background Concentration in Soil (ppm)	Surficial Mobility	Use in Exploration
As	10	Mobile, Fe scavenged	Pathfinder especially for Au
Au*	1	Low	Au deposits
Mn	300	Moderate, high at low pH	Scavenges Co, Zn, Ag
Mo	3	Moderate to high pH > 10	Wide use
Ni	17	Low, scavenged	Wide use
Pb	15	Low	Wide use
Se	0.3	High	Little use
U	1	Very high, organic scavenged	Determined in water
V	55	Moderate?	Little use

* Unit of concentration in ppb
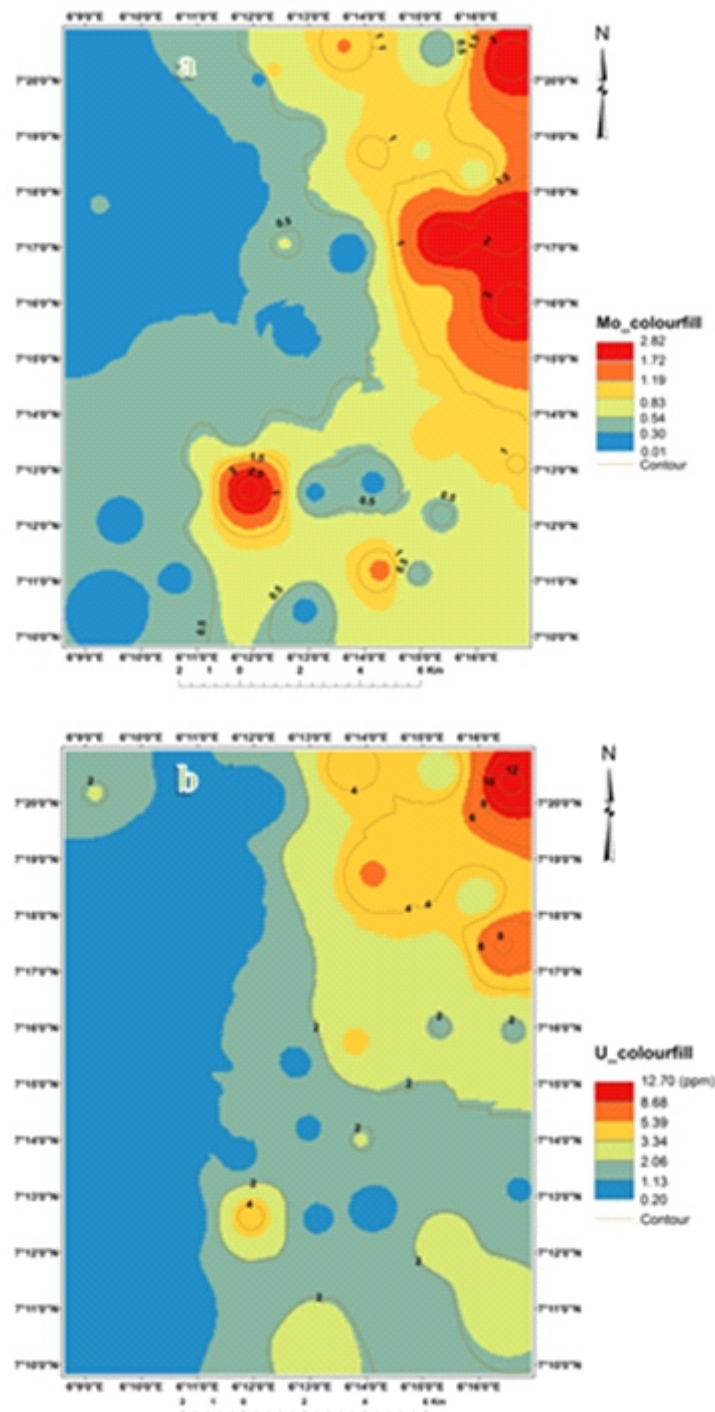
Figure 6: Geochemical distribution maps of (a) Mo and (b) U in the soils of Dagbala-Atte District.

DISCUSSION

Univariate Statistical Analysis

The aim of geochemical exploration is to delineate significant anomalies. Anomalies are outlined by statistically grouping data using univariate statistics. The best way of statistically grouping data is graphical examination using histograms and box plots (Howarth, 1984; Garrett, 1989).

Histograms

Histogram is a graphical means of presenting distribution, which commonly exhibits shape similar to theoretical frequency distributions. The histograms of the raw data evinced positive skewness of the elements in varying degrees Figure 4(a) while the plots of log-transformed data manifested little or no skewness, which

signifies that the distribution of the elements are log-normal (Figure 4b). Breaks in distribution of the raw data occurred at 1.75% for Fe, 20 ppm for As, 1.5 ppm for Mo, 0.7 ppm for Se, 8.75 ppm for U and 87.5 ppm for V. The breaks in distribution allude to mixture of populations, however only As maintained break in distribution in the log-transformed data histograms.

Box plots
The box plot is commonly used to display some statistical parameters in a graphical form (Turkey 1977). As long as the scale of presentation is logical, the box plot gives a fast visual estimate of the frequency distribution. The box plots of the raw data (Figure 5a) exhibited longer whiskers above the mean and shorter ones below it, revealing wide variation of the geochemical data, which suggests a non-normal situation. However, the log-transformed dispersion box plots (Figure 5b) gave a more refined dataset with both the maximum and minimum values evenly distributed about the mean value indicating log-normal distribution of the geochemical data. This provided a data set with negligible variance that aided data interpretation. Each of the raw and logarithmically transformed data plots revealed the number of samples with anomalous concentrations of elements, called outliers in the box plots (Figures 5a and 5b).

Selection of threshold
Table 3 gives the summary of descriptive statistics, and other parameters, drawn from the histograms and the box plots for the 10 elements. Since univariate statistics revealed that the geochemical data in the study area are log-normally distributed, log-data set was also used for the calculation of thresholds (Thr.) from histograms and boxplots, respectively using the formulae:

Mean + 2*St. Dev. (Thr. 1) _____ (1)
and Q3 + 1.5*IQR (Thr. 2) _____ (2)

Equations 3 and 4 were used to resolve the values from logarithmically transformed data to their

$10^{(Mean + 2*St. Dev.)}$ _____ (3)
and $10^{(Q3 + 1.5*IQR)}$ _____ (4)

raw data equivalents. However, Thr. 1 was favored for this study as it gave much lower threshold values for all the elements except Mn and Se that

have related values of threshold in the two models of threshold calculation (Table 3). Though, the choice of this set of lower threshold values for the elements could sometimes lead to misconception of false anomaly as due to mineralization, if not adequately correlated with geological data. However, it increases the chance of having more sites that can be considered anomalous for further investigations.

Multivariate Statistical Analysis
Multivariate statistical analysis allows an opportunity to examine the relationship among the elements (Moon, 1986). The chief assumption fundamental to the application of the multivariate methods of CM and FA is for the data to follow normal distribution. As discovered through the univariate statistical analysis, the raw datasets of the elements used in this study are non-normal, but their logarithmically transformed datasets are normal. Therefore, the logarithmically transformed data are used in the determination of CM and FA. Another important assumption in multivariate statistics is that the element to be used must not contain more than 30 % of the values of the censored data below the analytical detection limits (DLs) (Sadeghi *et al.* 2015). Hence, Se that was below DLs in 15 of the 49 sample location sites was exempted from the CM and FA. For elements As, Au and Mo, which contain only 1, 6 and 1 censored data, values equal to 66 % of their lower DLs were applied for the computation of CM and FA. The CM and FA were built only for the logarithmically transformed analytical data of the nine elements (Fe, As, Mn, Mo, Ni, Pb, U, V and Au), that met the requirements.

Correlation matrix
Correlation coefficients of nine elements (Fe, As, Mn, Mo, Ni, Pb, U, V and Au), in the Dagbala-Atte soil (Table 4) showed very strong correlation (r ≥ 0.75) between Fe-Mo, Fe-V, Mo-Pb and Ni-V; strong correlation (0.50 ≤ r < 0.75) between each of As-Fe, As-V, Fe-Ni, Fe-Pb, Fe-U, Mn-Pb, Mo-U, Pb-U and Pb-V and fairly strong correlation (0.25 ≤ r < 0.50) between each pair of As-Au, As-Mo, As-Ni, As-Pb, As-U, Au-V, Fe-Mn, Mn-Mo, Mn-Ni, Mo-V and Ni-Pb. The strong correlation observed between uranium and each of Fe, Mo and Pb may reflect primary association among the four elements. The correlation, generally vary

from fairly strong to very strong positive correlation between some pairs and weak negative correlation between other pairs. However, all the correlation coefficients between the elements were significant at 95 % confidence level and above. The association of Mo, Pb and U indicates the possibility of U occurrence in the granitic rocks of the study area (Rose *et al.,* 1991).

Factor analysis
The rotated equamax factor matrix presented in Table 5(a) afforded information on eigenvalues, which is the amount of the total data explained by each model and communalities. That is the amount of the total variability of each element explained in a given factor model for the factor model obtained. As shown in Tables 5(a) and (b), the element associations of Factor 1 is Mo-U-Pb-Fe-Mn, Factor 2 is Ni-V-Fe-As and Factor 3 is Au-Mn-As. Table 5 (a) shows that each factor consists of significant contributions from certain variables and less important to negligible contributions from others. The total variance of the three-factor model is 81.5 % (Table 5b).

In summary, Factor F-1 is the most relevant to the present study as it is the only factor that contains uranium among the three factors. It is the most pronounced factor and accounts for 33.5 % of the three-factor model in the area. It is interpreted to indicate probable Mo-U-Pb association characteristic of U mineralization in granitic rocks (Table 2). The presence of Fe and Mn in this factor raises the possibility of scavenging action of the metals on or co-precipitation with other elements associated with them in the factor model. This is owing to the fact that the residual soil environment is a secondary geochemical environment where either of those activities can easily take place. However, the relatively low correlation coefficient (0.442) between Fe and Mn (Table 4) suggests that the likelihood of environmental influence involving the well-known sympathetic behavior of Fe and Mn in the secondary (soil) geochemical environment is low. If these propositions are correct, one can surmise that the association of Fe and Mn with other elements in the factor model is probably not influenced by the scavenging action of or co-precipitation with Fe and Mn in the secondary (soil) environment but rather more profoundly controlled by inheritance of the elements from the bedrock from which the residual soil is derived.

Geochemical Distribution of U and its Associated Elements (Mo and Pb) in the Study Area
The geochemical distribution maps of the elements in the soils of the district (Figure 6) have been used to explain the distribution of U and its associated trace elements (Mo and Pb) in the residual soils. Adepoju *et al*. (2018) and Adesiyan *et al*. (2014) observed that the spatial distribution maps of the elements in residual soil are useful guides to possible sources of anomalous concentration of elements. Therefore, the geochemical distribution maps of Mo, Pb and U in the district were superimposed on the geological map with the residual soil sample locations (Figure 2). This was carried out in order to correlate the distribution of the elements in the residual soil of the district with their possible bedrock. To determine the significance of the anomalous sites selected on the basis of the threshold values for the elements, threshold values were compared with the background concentrations of the elements in the World's soils (Table 6) overlying similar rocks (Levinson, 1980; Rose *et al.,* 1991). Where the concentration of any element in an anomalous site is lower than the background value in the World's soils (Table 6) such anomalous site was considered insignificant.

The distribution of Mo in Dagbala-Atte District (Fig. 6a) showed that Mo is fairly widely distributed in the study area being present in detectable amounts in 48 out of 49 samples and below the lower limit of detection of 0.01 ppm in just one sample. It ranges in concentration from 0.04 to 2.82 ppm with a mean value of 0.68 ppm. At the selected threshold value of 2.98 ppm (Table 2), no anomalous Mo value exists in the area. A comparison of the threshold value of Mo (2.98 ppm) in Dagbala-Atte District soils with its average background in the World's soils (3 ppm) (Tables 3 and 6) indicated that the value in the study area is rather low. Nevertheless, there exist some significantly high Mo concentrations at sites DPS01 (2.25 ppm), DPS15 (2.5 ppm), DPS16 (2.46 ppm), DPS28 (2.16 ppm) and DPS38 (2.82 ppm). All these sites of highest Mo concentrations lie within the granitic gneiss, except DPS28 and

DPS38 that occurred within the quartz biotite schist lithology (Figure 2). The distribution map of Mo (Figure 6 a) showed three areas of high Mo concentrations, one small circular shape in the far north eastern part of the district on granite gneiss, the second fairly extensive in the far east central part of the district on granite gneiss and granite, and the third small circular in the south central part of the district on the biotite schist, which may likely be a false anomaly resulting from fluvial transportation of sediments and infiltration of Mo laden fluid.

The distribution of Pb in the study area is widespread. It is concentrated in all the 49 samples analyzed. The Pb contents ranged from 1.99 to 26.94 ppm with a mean of 11.55 ppm. With the selected threshold of 31.0 ppm, no anomalous values exist for Pb in the study area. However, fairly high concentrations occur at sample sites DPS15 (24.99 ppm), DPS28 (20.41 ppm), DPS44 (20.2 ppm) and DPS46 (26.94 ppm). All these sites of highest Pb concentration values (DPS15, DPS28, DPS44 and DPS46) are underlain by granitic rocks (mainly granitic gneiss) in the eastern and southeastern parts of the district (Figure 2). Comparison of these high Pb sites with the background values of Pb in the world soils (15 ppm), showed that the values at these sites are significant. The distribution map of Pb revealed four areas of highest concentrations, two fairly large circular areas underlain by granitic gneiss in the eastern and southeastern parts of the district and two small circular areas in the eastern part underlain by granite and in the southeastern part underlain by granitic gneiss.

Uranium contents ranged from 0.2 ppm to a peak value of 12.7 ppm with a mean of 1.3 ppm. With the selected threshold at 8.6 ppm, one anomalous value occurs at site DPS01 (12.7 ppm) with two other fairly high U values at sites DPS12 (5.9 ppm) and DPS15 (8.5 ppm). These sites with anomalous values in the northeastern and central eastern parts of the district are underlain by granitic gneiss (Figure 2). Uranium distribution map (Figure 6b) shows a strongest anomalous area at the northeastern corner of the district. The mean value obtained (1.1 ppm) as compared with the background concentration of U in soils (Table

6) shows that the distribution of U is fairly high in the study area and that the anomalous value obtained (12.7 ppm) is significant and may be due to U mineralization in the district. Thus, the numerous granite-pegmatite veins in the granitic gneisses of the northeastern part of the district, around Dagbala, may be U-bearing giving the associated anomalous concentrations of Mo, U and Pb in the same area. This disium as vein-type mineralization in Nigeria (Adekanmi *et al.*, 2007; Funtua and Okujeni, 1996; Ige *et al.*, 1994). Uranium-bearing pegmatites have been reported to occur in many countries all over the world (e.g. Guo *et al.*, 2021; Bourret, 1988; Carter, 1984; Adams *et al.*, 1980)

SUMMARY AND CONCLUSION

Pedogeochemical survey for exploration of U mineralization was undertaken in Dagbala-Atte District in the Igarra Schist Belt of southwestern Nigeria. Histograms and box plot diagrams of U, As, Fe, Mn, Mo, Ni, Pb, Se, V and Au compositions of residual soils showed that they are all log-normally distributed and are used for the determination of threshold values. Threshold values for Fe, As, Mn, Mo, Ni, Pb, Se, U, V and Au, are 9.47 %, 10.8, 1589, 2.98, 45.6, 31.0, 0.68, 8.59 and 122 ppm and 10.6 ppb, respectively. Strong correlation between uranium and each of Fe, Mo and Pb indicated close primary association among the four elements. Factor analysis revealed U, Mo, Pb, Fe and Mn association, which supports possible presence of U in granitic rocks in the study area (Rose *et al.* 1991). Geochemical distribution map showed U, Mo and Pb association in the northeastern, east-central and southern part of the study area. Strongest U anomaly was recorded in the northeastern part of the district. The suspected U mineralization in Dagbala Atte District is linked with the area underlain by granitic gneisses intruded by quartzo-feldsparthic veins in the northeastern part of the district.

In conclusion, the numerous granite-pegmatite veins in the granitic gneiss around Dagbala area in the northeastern part of the area might be uranium bearing. Therefore, copious geological study of these pegmatite veins is recommended.

REFERENCES

Adams, J.W., Arengi, J.T. and Parrish, I.S. 1980. Uranium- and thorium-bearing pegmatites of the United States. Unpublished report, The U.S. Department of Energy, Colorado. DOI:10.2172/5201124.

Adekanmi, A. A., Ogunleye, P. O., Damagum, A. H. and Olasehinde, O. 2007. Geochemical map of uranium distribution in the residual soil of GRN Cell Number N08 E05, unpublished report, *Nigerian Geological Survey Agency*, Abuja.

Adepoju, M.O. 2019. Geochemical soil survey for base and precious metals in Dagbala-Atte District, Southwestern Nigeria. *International Journal of Geosciences* 10: 141-159. https://doi.org/10.4236/ijg.2019.102009.

Adepoju, M.O. 2017. Geological and geochemical exploration studies in Dagbala-Atte district in Igarra Schist Belt, Southwestern Nigeria. Unpublished Ph.D. thesis, FUTA, Nigeria, 323 p.

Adepoju, M.O., Adekoya, J.A. and Awoniran, D.R. 2019. Exploration for ferrous metals using geochemical soil survey in Dagbala-Atte district, Southwestern Nigeria. *International Advanced Research Journal in Science, Engineering and Technology* 6 (3): 100-111. https://doi.org/10.17148/IARJSET.2019.6318.

Adepoju, M.O., Adekoya, J.A. and Odeyemi, I.B. 2018. Statistical evaluation of soil geochemical data from Dagbala-Atte district in Igarra Schist Belt, Southwestern Nigeria. *Geoinformatics and Geostatistics*: An Overview 6: 4.

Adepoju, M.O. and Adekoya, J.A. 2011. Reconnaissance geochemical study of a part of Igarra Schist Belt, Southwestern Nigeria. *Ife Journal of Science* 13: 75-92.

Adepoju, M.O. and Adekoya, J.A. 2008. Statistical analysis of reconnaissance geochemical data from Orle District, Southwestern Nigeria. *Global Journal of Geological Science* 6: 63-74.

Adesiyan, T.A., Adekoya, J.A., Akinlua, A. and Torto, N. 2014. Statistical studies of soil geochemical data from Gbongan-Odeyinka area, Southwestern Nigeria. *Geoinformatics and Geostatistics*: An Overview 2: 1.

Appleton, J. D., Johnson, C. C., Ander, E.L. and Flight, D.M. A. 2013. Geogenic signatures detectable in topsoils of urban and rural domains in the London region, UK, using parent material classified data. *Applied Geochemistry*, vol. 39, 169-180. DOI: 10.1016/j.apgeochem.2013.07.010

Bourret, W. 1988. Uranium-bearing pegmatites of the Antsirabe-Kitsamby District, Madagascar. *Ore Geology Review* 3 (1-3): 177-191.

Carter, J.D. (1984): Mortimer Hills pegmatite uranium prospect a Rossing Type uranium deposit in the Gascoyne Province. International Atomic Energy Agency (IAEA) Report, vol. 17(1), Issue 8, pp. 27-31.

Chaudry, M.A., Donze, M., Tabrez, A.R. and Inam, A. (2001): Geochemical soil survey for the exploration of uranium ore deposits, NE Vogelkop, Irian Java, Indonesia. Journal of Applied Sciences, 2: 948-945

Dada SS (2006) Proterozoic Evolution of Nigeria. In Oshin O (ed.): The basement complex of Nigeria and its mineral resources. Akin Jinad and Co. Ibadan, Nigeria, pp. 24-44.

Egbuniwe, I.G. and Ocan, O.O. 2004. Selection of fieldwork areas for teaching/training: Igarra Area as an example. Proceedings of Field Mapping Standardization Workshop, Ibadan University Press, Ibadan, 79-95.

Funtua, I.I. and Okujeni, C.D. 1996. Element distribution patterns in the uranium occurrence at Mika, northeastern Nigeria. *Chemie der Erde*, Gustav Fischer Verlag, Jena, 245–260.

Garrett, R.G. 1989. The role of computers in exploration geochemistry. in: Garland, G.D. (ed.) *Proceedings of Exploration '87*, spec. vol. 3, 586–608. *Ontario Geological Survey*, Toronto.

Guo, G., Bonnetti, C., Zhang, Z., Li, G., Yan, Z., Wu, J., Wu, Y., Liu, X. and Wu, B. 2021. SIMS U-Pb dating of uraninite from the Guangshigou uranium deposit: Constraints on the Paleozoic pegmatite-

type uranium mineralization in North Qinling orogen, China. *Minerals* 11: 402. https://doi.org/10.3390/ min11040402.

Hockey, R.D., Sacchi, R., de Graaff, W.P.F.H. and Muotoh, E.O.G. 1986. The geology of Lokoja-Auchi Area: Explanation of 1:250,000 Sheet 62. *Geological Survey of Nigeria Bulletin* No. 39, 71 p.

Howarth, R.J. 1984. Statistical applications in geochemical prospecting: a survey of recent developments. *Journal of Geochemical Exploration* 21:41-61.

IAEA 2001. Analysis of Uranium Supply to 2050. IAEA-SM-362/2, Vienna, Austria. Ige, T.A., Okujeni, C.D., Elegba, S.B. (1994): Distribution pattern of REE and other elements in the host rocks of the Gubrunde uranium occurrence, northeastern Nigeria, J. Radioanal. Nucl. Chem. 178, 365–373.

Levinson, A.A. 1980. Introduction to Exploration Geochemistry. Applied Publishing, Wilmette, IL., USA.

McCurry, P. 1976. The geology of the Precambrian to lower Paleozoic rocks of northern Nigeria—A Review. in: Kogbe, C.A. (ed.), Geology of Nigeria, Elizabethan Publishing, Lagos, 15-59.

Moon, C.J. 2006. Exploration Geochemistry. in: Moon, C.J., Whateley, M.E.G. and Evans, A.M. (eds.), Introduction to Mineral Exploration, 2nd Edition, Blackwell Publishing, pp. 155-178.

Odeyemi, I.B. 1988. Lithostratigraphy and structural relationships of the upper Precambrian metasediments in Igarra area, southwestern Nigeria. in: Oluyide, P.O., Mbonu, W.C., Ogezi, A.E., Egbuniwe, I.G., Ajibade, A.C. and Umeji, A.C. (eds.), Precambrian Geology of Nigeria, Publ. GSN, 111-125.

Power, M.J., Hattori, K., Sorba, C. and Potter, E.G. 2012. Geochemical anomalies in the soil and uppermost siliciclastic units overlying the Phoenix uranium deposit, Athabasca Basin, Saskatchewan; Geological Survey of Canada, Open File 7257, 36 p. http:doi.10.4095/291981

Rose, A.W., Hawkes, H.E. and Webb, J.S. 1991. Geochemistry in mineral exploration, 3rd edition, Academic Press, London, 711 p.

Sadeghi, M., Billay, A. and Carranza, E.J.M. 2015. Analysis and mapping of soil geochemical anomalies: implications for bedrock mapping and gold exploration in Giyani area, South Africa. *Journal of Geochemical Exploration* 154: 180-193. https://doi.org/10.1016/j.gexplo.2014.11.018

Tukey JW (1977) "Exploratory Data Analysis," 1st edition, Addison-Wesley, 183 p.

Zhang, B., Wang, X., Zhou, J., Han, Z., Liu, W., Liu, Q., Wang, W., Li, R., Zhang, B. and Dou, B. 2020. Regional geochemical survey of concealed sandstone-type uranium deposits using fine-grained soil and groundwater in the Erlian basin, north-east China. Journal of Geochemical Exploration, IF 3.353, *DOI: 10.1016/j.gexplo.2020.106573*